Determination of Mechanisms for the Irradiation of N-halamines

Jacob Mahaffey
Carthage College
10/31/12

Abstract:

N-halamines have been shown to be great antimicrobial agents. This is due to the regenerative properties of these molecules. The exposure of N-halamines to UVA radiation (315-400nm) has been shown to decrease the regenerative ability in these molecules. In order to solve this problem the mechanistic pathway must first be explained. By using ^{1}H NMR and DFT calculations, the most probable mechanism for photodegradation will be determined. An intermolecular radical interaction was observed for the molecules of interest. This interaction matched both ^{1}H NMR spectra and DFT calculations, which supports the proposed schemes.

Introduction:

N-halamines have been shown to be very good antimicrobials as both monomeric and polymeric coatings on certain materials[1, 2]. These molecules can be coated on solid surfaces such as glass, and on materials for medical use[3]. It has been shown that methyl substituted N-halamines are less reactive than phenyl substituted versions, and therefore the former is the center of this research[1]. The production of these antimicrobials is inexpensive, nontoxic, and environmentally safe[4].

These molecules display a regenerative ability that makes them very useful in many applications[5]. During use as an antimicrobial, these molecules naturally lose a halogen to destroy or inhibit enzymatic or metabolic processes[6]. This dehalogenation is counteracted when the molecules are exposed to solutions containing chlorine or bromine ions, allowing them to reform the original reactants[7]. One current application of coating materials with these molecules is water purification in developing countries[8]. Another application is use as medical

textiles, in which the molecules are bound to fabric as an antimicrobial agent [5].

Over time, the ability for these molecules to regenerate is reduced when exposed to UVA radiation (315-400nm, at .69 w/m^2)[9]. This is due to either rearrangement or removal of the chlorine atom from the nitrogen atom from a radical reaction. This problem must be addressed before large-scale application of this technology can be implemented. The first step is to determine exactly what causes the degeneration of these molecules. By understanding the mechanisms involved during the irradiation of these molecules, solutions to this problem can be found. The two specific N-halamines that were synthesized and studied in this research are shown in (figure 1). The first molecule (1) is 1-chloro-3,5,5-trimethylhydantoin, and the second molecule (2) is 3-chloro-1,5,5-trimethylhydantoin.

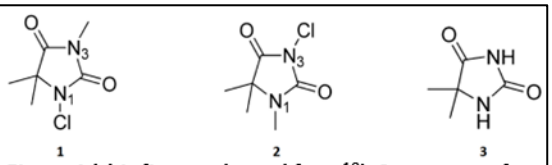

Figure 1 (this figure adapted from[10]): Structures of Hydantoins:
1-chloro-3,5,5-trimethylhydantoin(1), 3-chloro-1,5,5-trimethylhydantoin(2), and 5,5-dimethylhydantoin(3)

Both molecules were synthesized from the base reagent (3) 5,5-dimethylhydantoin. All of the original reagents were purchased from Fisher Scientific Inc. (Fair Lawn, NJ) or Aldrich Chemicals Inc. (Milwaukee, WI)[10]. The synthesis of molecule (1) starts with a methyl group replacing the hydrogen on the imide nitrogen. Then a chlorine atom was placed on the amide group. The synthesis of molecule (2) involved placing a protecting group on the imide nitrogen, and then the methyl group was added to the amide nitrogen. Finally the protecting group was removed and then a chlorine atom was added.

In order to find the mechanistic pathway of the irradiated N-halamines, ^{1}H NMR, and Density Functional Theory (DFT) will be used to compare theoretical and experimental results.

^{1}H NMR spectra of reactants, possible products, and final products of the irradiated molecules were given to show which products are produced, and the product ratios of both reactions studied.

DFT is a quantum chemical calculation that is used to find the Gibbs Free Energy of the transition states of possible reactions. DFT utilizes the Schrodinger Equation, which is used to model energies and locations of electrons[11]. DFT is time consuming and computationally extensive, therefore simplifications of the molecules and their transition states are applied[11]. The first simplification is to use electron density models to describe the location of the electrons[11]. The second assumption applied is that there is a singular and uniform force on these electrons [11] These assumptions simplify the Schrodinger Equation, and allow a computational calculation of the Gibbs Free Energy of Activation ($\Delta G^{\ddagger}$) (measured at the UB3LYP/6-311G++(2d,p) level). A basic energy diagram showing $\Delta G^{\ddagger}$ and Eyring's equation is illustrated in (figure 2).The energies that were calculated were these of the transition states for proposed mechanisms. The lower the energy of the transition state, the more likely the reaction occurs. From $\Delta G^{\ddagger}$, Eyring's equation can be used to calculate the rate constant for a reaction. This can be used to compare the probability associated with each reaction. This data will be compared to the ^{1}H NMR results to support, or reject the theorized mechanisms.

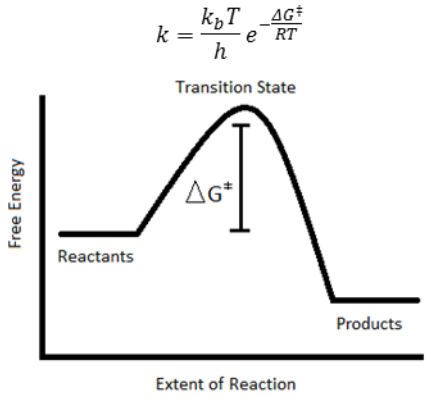

Figure 2: Energy Diagram/Erying's Equation: The Free Energy of Activation (ΔG‡) found in this experiments were determined by subtracting the Free Energy from the reactants from the Free Energy of the transition state. The equation represented above the diagram demonstrates how rate constants can be calculated from ΔG‡.

Free radical chemistry can be broken down into three parts: initiation, propagation, and termination. The initiation step occurs when a high energy source, such as UV light, cause a bond or pair of electrons to split into a single electron (radical). Propagation is the next step, and it is when one free radical reacts with another atom to transfer the radical to the other atom. The final step is termination, and this occurs when two radicals react to restore the electron pair or bond. Certain bonds are more likely than others to undergo radical reactions. One such bond is the N-Cl bond found in the starting molecules. Since molecules (1,2) lose functionality in the presence of UVA radiation, free radical mechanisms were the center of this study.

In order to determine the exact mechanism, both intermolecular and intramolecular radical mechanisms will be proposed. These will be compared with both the ^{1}H NMR spectra produced, and the DFT calculations. The mechanism that fits both results will be the most probable pathway that molecules (1,2) go through. This mechanism will give information into why these molecules are degrading in the presence of UVA radiation. Credit for the research used in this paper is given to *McCann, et al. at Department of Chemistry and Biochemistry, Auburn University*[10].

Results and Discussion:

The aim of this experiment is to determine the photodegradation mechanism for N-Halamine molecules (1,2) (figure 1) during exposure to UVA radiation. Both solid state and solution based products were studied. The theorized mechanisms and products contain both intermolecular and intramolecular interactions. By using solution phase NMR, and Density

Functional Theory (DFT), proper mechanisms can be assigned to match results found experimentally.

Initial tests of molecules (1) and (2) were done to determine the rates at which the hydantoins lost chlorine in the absence of UVA radiation. This experiment was accomplished by making weekly measurements, and monitoring the amount of chlorine ions in $CDCl_3$ solution or %weight by titration for remaining chlorine ions. The rates of dehalogenation are shown in (Figure 3). The graphs show that molecule (1) loses chlorine at a much slower rate than molecule (2). This result is expected due to the increased number of resonance structures that molecule (2) has. These resonance structures come from both carbonyl groups surrounding the chlorine containing nitrogen in molecule (2) as opposed to only one carbonyl group in molecule (1). The resonance in (2) stabilizes the dechlorinated form, and therefore the energy barrier to reach the unfavorable charged state is easier to overcome. This is the reason that the amount of chlorine remaining in both cases is greater for compound (1). By being dissolved in solution, the hydantoins experienced a greater rate for chlorine loss. This result could be due to intermolecular interactions with the polar solvent and the ions in solution due to intermolecular forces destabilizing the polar bonds in the hydantoins.

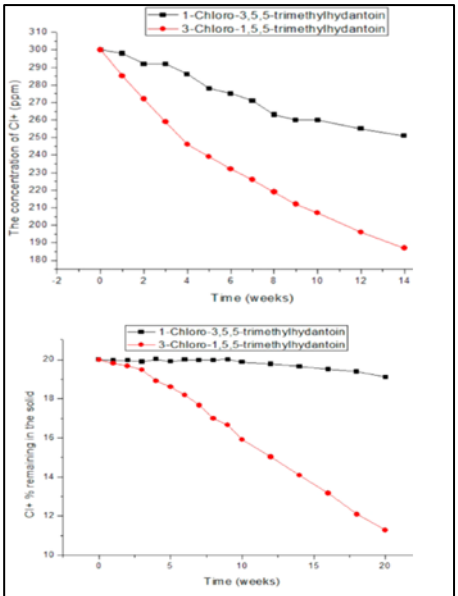

Figure 3[10]: Molecule 1 looses less chlorine in the absence of UVA radiation than molecule 2 in both solid state and water solutions. Top graph represents molecules 1,2 dissolved in water, and the bottom is solid state.

The dehalogenation of both molecules in the presence of UVA radiation is shown in (figure 4). It is important to note that this graph is on the time scale of hours as opposed to weeks as in the previous figure. The introduction of UVA radiation (at .69 w/m^2) to the molecules greatly reduces the amount of time that chlorine stays on the molecule. From this result, it is concluded that free radicals cause an increase in the oxidative dechlorination of both molecules (1,2). Figure 4 once again shows that molecule (1) loses chlorine at a much slower rate. This leads to the purpose of finding the mechanism that leads to this result for the irradiation of initial molecules.

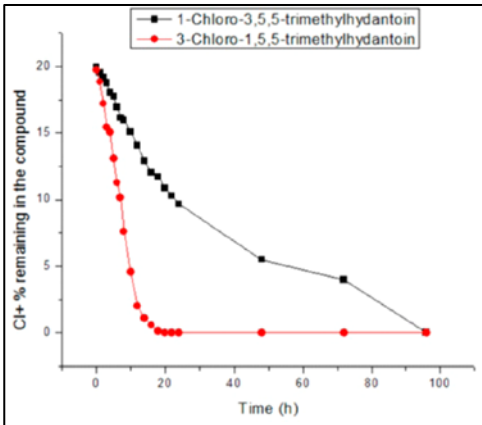

Figure 4[10]: Chlorine loss in the presence of UVA radiation for molecule(1) is shown to be less than the chlorine loss of molecule 2. The irradiation of both molecules sped up the dechlorination process. Molecule 1 still has roughly 55% of chlorine left when molecule 2 has lost all chlorine.

The proposed products produced by irradiating both molecules with UVA radiation are shown in (scheme 2). (1a) shows an exchange of the chlorine from the amide to the methyl group attached to the imide. (1b) shows the dehalogenation of molecule(1). (1c) is the final possibility, and shows the chlorine being exchanged from the N1 atom to one of the methyl groups on the C5 carbon. The proposed products for molecule(2) under UVA conditions are the same, only with the chlorine starting on the imide. These possible products show the only possible outcomes of

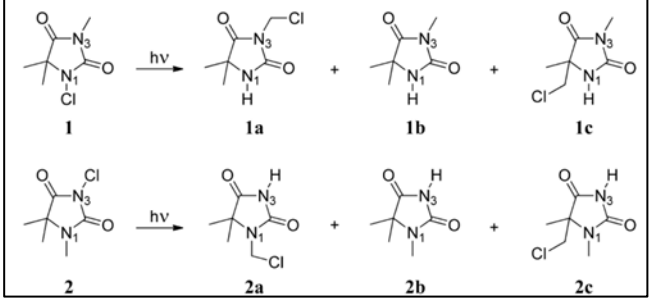

Scheme 2[10]: Proposed products of molecules (1,2) after exposure to UVA radiation. Product names: 3-chloromethyl-5,5-dimethyl hydantoin(**1a**), 3,5,5-trimethyl hydantoin(**2b**), 5-chloromethyl-3,5-dimethyl hydantoin(**1c**), 1-chloromethl-5,5-dimethyl hydantoin(**2a**), 1,5,5-trimethyl hydantoin(**2b**), 5-chloromethyl-5-methyl hydantoin(**2c**).

chlorine transfer in molecules (1,2). ^{1}H NMR spectra of these pure theorized products were produced, and used as reference spectra for the ^{1}H NMR spectra for the products of molecules (1,2) after exposure to UVA radiation. By comparing these spectra, the products produced should line up with the reference spectra. This data was used as a guideline for the proposed mechanisms.

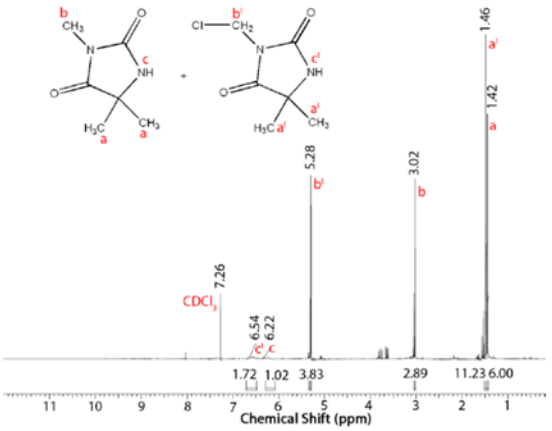

Figure 6[10]: Product peaks show peaks corresponding to products 1a and 1b for the radiation of molecule(1). ^{1}H NMR of the irradiated molecule 1 in CDCL3. The peaks are labeled with the corresponding hydrogens. Product 1b (left) and product 1a (right) were the only two products found in solution. Integrated peak values show product ratios of 1a:1b.

The ^{1}H NMR spectrum for the photodecomposition of compound (1) in CDCl3 solution is shown in (figure 6). The assignments for each peak are given in the figure. There are more peaks than in one of the control NMR spectra because there are multiple products for the irradiation of molecule (1). There are also several smaller peaks; these are too small to be considered a major product. This result shows that there are some impurities in the experiment conducted. In this case, only two products were found in the solution after irradiation. The control NMR spectra can be compared to see which match the final product NMR. By doing this, molecule (1b) and molecule (1a) are the only two products present in the final solution. This result shows that the mechanism that results from the radiation of molecule (1) does not allow for the production of molecule (1c).

The product ^{1}H NMR spectrum for molecule (2) is given in (figure 7). These peaks have also been labeled. By lining up the product spectra for molecule (2), it is shown that only two products (2a, 2b) are present. This result means that none of molecule (2c) was produced. There are also some impurity peaks in this spectrum as well. Based on the NMR results, the mechanisms must not produce molecule (1c) or (2c).

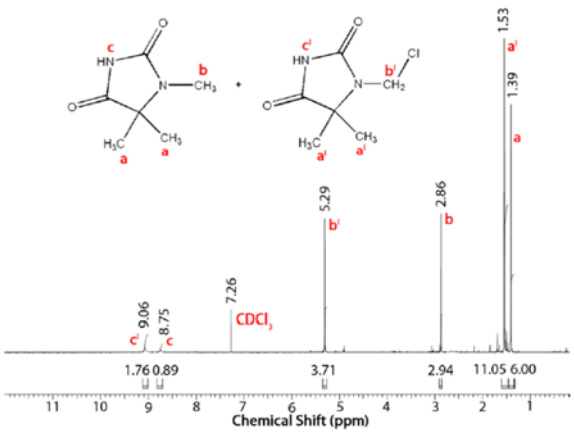

Figure 7[10]: Product peaks show peaks corresponding to products 2a and 2b for the radiation of molecule(2). ^{1}H NMR of the irradiated molecule 2 in CDCL3. The peaks are labeled with the corresponding hydrogens. Product 2b (left) and product 2a (right) were the only two products found in solution. Integrated peak values show product ratios of 2a:2b.

The product ratios were determined by comparing the integrals of the peaks corresponding to similar hydrogens in (figures 6,7). For example peaks a and a' can be compared to show the product ratio. It is easiest to use the first major peak because the ratio is already in whole numbers. The product ratio for both 1a:1b and 2a:2b in CDCl3 is 11:6. The product ratios for the irradiation of the solid state can be found in (table 1). These values are not similar, and were not discussed in further detail in the article.

Table 1(this figure adapted from[10]): Product Ratios of Solid State and $CDCl_3$. Ratios calculated from integrated peaks of ^{1}H NMR spectra of molecules(**1,2**) after exposure to UVA radiation.

Product Ratio	**1a:1b**	**2a:2b**
Solid State	10:1	1.5:1
In $CDCl_3$	11:6	11:6

Next, theorized mechanisms were explored to find the most likely pathway. Each transition state was analyzed by DFT (Density Functional Theory) to give the $\Delta G^{\ddagger}$ values. The mechanisms with the lowest $\Delta G^{\ddagger}$ are the most probable. These values will be matched with the

results of the NMR data to see which mechanism best fits this reaction.

When molecules (1,2) are exposed to UVA radiation, the highly reactive nitrogen-chlorine bond can break resulting in a single electron on the nitrogen and the chlorine which is shown in the first step of (scheme 3). This is the initiation step for all mechanisms being studied. The first mechanisms being studied are intramolecular reactions. Because of this, the free radical must propagate between atoms in an individual molecule throughout the reactions. The first possible mechanism shows the formation of (1a) (one of the products found in the ^{1}H NMR spectrum), and (1c) (a product not found in the ^{1}H NMR spectrum) is shown by (scheme

Scheme 3 (this figure adapted from[10]): Intramolecular Mechanisms. Product(1a) is formed when the radical is transferred across the imide to the N3 methyl group. The transition energy for this is 40.4 kJ/mol. Product(1a) is formed through a direct transfer from the N1 radical to one of the methyl groups on the C5 atom. This has a transition energy of 36.4 kJ/mol.

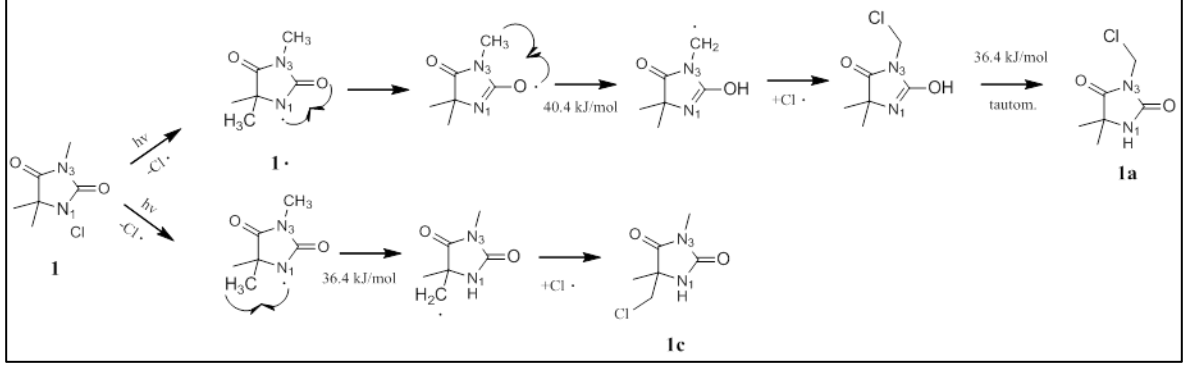

3). The production of (1a) goes as follows. The initiation step occurs when the nitrogen chlorine bond is split into radicals by the UVA radiation. The radical nitrogen can then react with the neighboring carbonyl group to propagate the radical to the oxygen atom. From here, the free radical propagates to the methyl group on the N3 atom in an intramolecular reaction. This radical then gets terminated when a radical chlorine reacts with the methyl radical. There is then a tautomerization to remake the carbonyl group. The $\Delta G^{\ddagger}$ values for the transition state of the intramolecular reaction and the tautomerization are 40.4 KJ/mol and 36.4 KJ/mol

respectively as determined by DFT.

The lower mechanism in (scheme 3) has the same initiation step as the previous mechanism. Then the N1 radical plucks a hydrogen from one of the methyl groups on the C5 atom during the propagation step. A radical chlorine then terminates the radical reaction. This reaction leaves us with the product (1c). During this reaction, the transition energy from the intramolecular interaction was 36.4 KJ/mol. This value is less than the transition state energy found in the previous mechanism, which would mean that the later mechanism is a more favorable reaction. The ^{1}H NMR spectrum showed that no (1c) was found, therefore this intramolecular mechanism is unlikely, and a new mechanism must be proposed to account for the products found.

Scheme 4[10]: Intermolecular Mechanism for Production of Products(1b,1c). Product(1b) is formed through transfer of **1** and **1** , this leaves the radical in position to be terminated leaving (1c). The formation of these products have a transition energy of 24.3 kJ/mol.

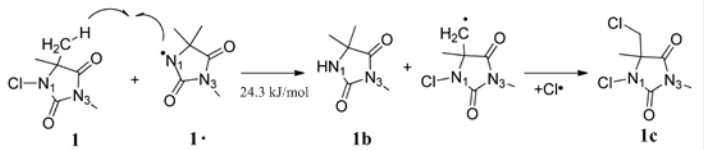

Another possible mechanism is shown in (scheme 4). This is an intermolecular reaction. The initiation step is the same as the first two mechanisms, in which the nitrogen-chlorine bond is split into radicals. This molecule then reacts with an unreacted molecule (1) at one of the hydrogens on one of the methyl groups on the C5 atom. This results in the production of product (1b) and a molecule (1) with a free radical on one of the C5 methyl groups. The $\Delta G^{\ddagger}$ value associated with the transition state of this reaction is calculated to be 24.3 KJ/mol. This reaction has a lower $\Delta G^{\ddagger}$ than the first two pathways examined, and therefore this is a more likely interaction. The free radical is then terminated by a radical chlorine. This

produces product (1c), which is an invalid mechanism based on the ^{1}H NMR.

Scheme 5 (this figure adapted from[10]): Intermolecular Mechanisms Producing(1a,1b). The initial step shows the production of (**1b**) and after termination, 1-chloro-3-chloromethyl-5,5-dimethyl hydantoin. This molecule is then irradiated, and is used for mechanisms **A**, **B**, and **C**. These mechanisms only produce **1a**, and **1b** along with molecules used in the initial line of the mechanism. The determining Free Energy is in the first step, and calculated to be 19.9 kJ/mol.

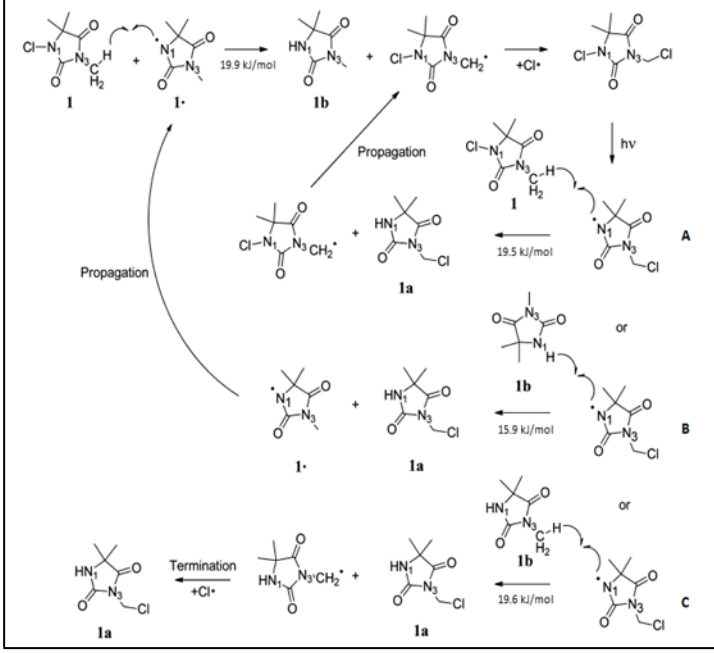

Other intermolecular reactions are shown in (Scheme 5). The initiation step is the same as all of molecule (1) reactions thus far. This free radical then propagates to the N3 methyl group of an unreacted molecule (1). This transition energy was calculated to be 19.9 KJ/mol. Product (1b) was then formed, along with molecule (1) with a free radical on the methyl group on the N3 atom. This reaction is terminated by another radical chlorine to produce 1-chloro-3-chloromethyl-5,5-dimethylhydantoin (possible contamination found in ^{1}H NMR). Now that this intermediate product has been formed, the UV light can create a radical on the N1 atom while retaining the chlorine on the N3 atom. This is the induction for three different pathways (A,B,C). All of these mechanisms are through intermolecular interactions. Mechanism A shows the production of product (1a). (1a) is produced when the newly formed radical reacts with an unreacted molecule (1). This produces product (1a), and the reactant found during previous step which can go back through pathways A, B, and C. This reaction has a $\Delta G^{\ddagger}$ value of 19.5 KJ/mol. The second possible reaction involving the N1 radical molecule once again produces product (1a). This reaction occurs when the N1 radical reacts with the hydrogen on

the N3 atom from product (1b) (produced during the first step). This step produces both product (1a) and one of the first reactants of the overall mechanism. The transition in this reaction has a $\Delta G^{\ddagger}$ of 15.9 KJ/mol. Pathway C also produces the product (1a). This pathway occurs when the N1 radical reacts with the methyl group attached to the N3 molecule of product (1b). This produces product (1a) and a radical that when terminated with a chlorine atom produces more (1a). The $\Delta G^{\ddagger}$ of this transition state is 19.6 KJ/mol. Product (1b) is as an intermediate in the production of product (1a). This results shows that more of product (1a) should be produced than (1b), which is consistent with product ratios found in table 1.

This last reaction has a highest predicted $\Delta G^{\ddagger}$ value of 19.9 KJ/mol. This occurs in the first step. The lowest $\Delta G^{\ddagger}$ of the previous mechanisms produced (1c) in (scheme 4) was 24.3 KJ/mol. The gap between these values is large enough to conclude that the reaction in (scheme 4) would almost never occur, and the reaction in (scheme 5) is the more probable pathway that molecule (1) follows. This result supports the NMR spectrum that only showed evidence of products (1a, 1b). This conclusion comes from the Eyring's Equation, which can be used to compare rate constant values (k) from $\Delta G^{\ddagger}$ values. To compare, 19.9 KJ/mol:24.3 KJ/mol converts to a reaction rate ratio of .169. This means that the reaction with the activation energy of 19.9 KJ/mol is six times faster than the reaction with the activation energy of 24.3 KJ/mol.

The proposed mechanisms for molecule (2) are very similar to those for molecule (1). There is a slight difference in the resonance structures found for the initial free radical. These resonance structures occur because the free radical can shift between both carbonyl oxygens along with the N3 atom freely. These resonance structures place the free radical close enough to methyl groups both on the C5 atom and the N1 molecule for a reaction to occur. This

arrangement causes an intramolecular interaction, and produces only (2a, 2c). These reactions have a very high $\Delta G^{\ddagger}$ for their transition molecules. Since the NMR showed only (2a, 2b), this intramolecular interaction can be ruled out.

This leaves only intermolecular reactions for the mechanism for molecule (2). The first mechanism studied is a direct transfer of the radical from the N3 atom of one molecule (2) to one of the C5 methyl groups. This produces the product (2b) and through the termination step, product (2c). The transition state for this reaction has a $\Delta G^{\ddagger}$ of 18.9 KJ/mol. Since (2c) is produced in this step, another mechanism must be explored.

Scheme 7 (this figure adapted from[10]): Intermolecular Mechanism producing(2a, 2b). The initial step shows the production of (**2b**) and after termination, 1-chloromethyl-3-chloro-5,5-dimethyl hydantoin. This molecule is then irradiated, and is used for mechanisms **A**, **B**, and **C**. These mechanisms only produce **2a**, and **2b** along with molecules used in the initial line of the mechanism. The determining Free Energy is in the first step, and calculated to be 18.5 kJ/mol.

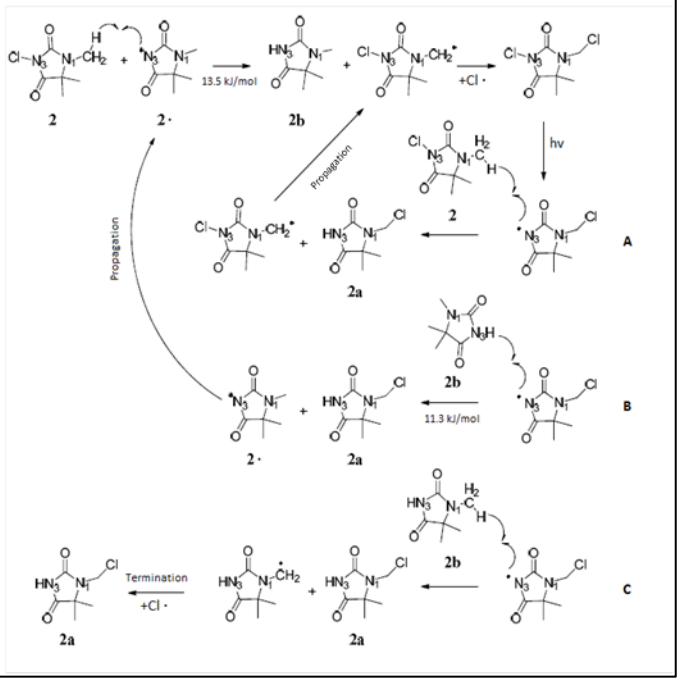

The other proposed intermolecular mechanisms are given in (Scheme 7). These mechanisms are similar those that molecule (1) followed. The only difference from molecule (1) is that the initial molecule has the radical on the N3 atom with the first propagation to the N1 methyl group. The $\Delta G^{\ddagger}$ for the transition state of this step is 13.5 KJ/mol. The only $\Delta G\ddagger$ that could be calculated for the three different sub-pathways was for the middle one, and it was 11.3 KJ/mol.

These ΔG‡ values are both under the 18.9 KJ/mol value seen in the mechanism that produced the (1c) product. This difference is large enough to assume that (scheme 7) is the only plausible mechanism for molecule (2). This result is supported by the observation that the only two products that were found in the ^{1}H NMR spectrum were (2a, 2b). The $\Delta G^{\ddagger}$ values for the different pathways show that more of product (2a) should be produced over (2b). This result is consistent with the product ratios from (table 1).

(Schemes 5,7) show the most probable mechanisms for the photodecomposition of the N-halamines being studied. These schemes were determined by both ^{1}H NMR and $\Delta G^{\ddagger}$ evidence. The agreement of both areas gives very strong evidence that the proposed schemes are accurate. Now that these schemes are known, possible work for finding ways to block the effects of UVA radiation can be done. This information should help in further research with these molecules. If the molecules can be modified to block the photodecomposition, these molecules can be used as a better antimicrobial agent.

The largest $\Delta G^{\ddagger}$ reported for molecule (1) during the most likely mechanism is 19.9 kJ/mol. The largest $\Delta G^{\ddagger}$ for molecule (2) was reported at 18.5 kJ/mol. These energies are directly related to the rate limiting step for the loss of chlorine in these molecules. Since the transition state energy of molecule (2) is less than that of molecule (1), molecule (2) is able to lose the chlorine easier than molecule (1). This should be expected based figures 3 and 4.

Conclusions:

Scheme 5 and scheme 7 show the best fitting mechanism for molecule (1) and molecule (2). These mechanisms are supported by the ^{1}H NMR spectra for the photodecomposition, and

the $\Delta G^{\ddagger}$ values of the transition states. These mechanisms are also supported by the product ratios found in (table 1). These schemes show that both of the studied molecules go through an intermolecular reaction when exposed to UVA radiation. The graphs of the decomposition of both molecules showed that molecule (1) is more stable than molecule (2). This conclusion was also supported by the lower energies for the transition states of the products of molecule (1) over molecule (2). The higher retention rate of molecule (1) is due to the resonance stability of molecule (2) when dehalogenated. The $\Delta G^{\ddagger}$ values associated with both transition states of the N-Cl radicals show that molecule (1) is more stable in the presence of UVA radiation. This stability comes from the lack of resonance forms that the molecule is capable of producing. By creating a larger transition energy, molecule (1) would be even more stable under UVA radiation. This change could be made by altering the substituents on the C5 atom to try to stabilize the N-Cl bond.

References

1. Kocer, H. B.; Worley, S. D.; Broughton, R. M.; Acevedo, O.; Huang, T. S., Effect of Phenyl Derivatization on the Stabilities of Antimicrobial N-Chlorohydantoin Derivatives. *Industrial & Engineering Chemistry Research* **2010,** *49* (22), 11188-11194.
2. Sun, Y.; Sun, G., Novel Refreshable N-Halamine Polymeric Biocides: N-Chlorination of Aromatic Polyamides. *Industrial & Engineering Chemistry Research* **2004,** *43* (17), 5015-5020.
3. Madkour, A. E.; Dabkowski, J. M.; Nüsslein, K.; Tew, G. N., Fast Disinfecting Antimicrobial Surfaces. *Langmuir* **2008,** *25* (2), 1060-1067.
4. Chen, Y.; Zhong, X.-s.; Zhang, Q., Synthesis of CO2-Philic Polysiloxane with N-Halamine Side Groups for Biocidal Coating on Cotton. *Industrial & Engineering Chemistry Research* **2012,** *51* (27), 9260-9265.
5. Liu, S.; Sun, G., Durable and Regenerable Biocidal Polymers: Acyclic N-Halamine Cotton Cellulose. *Industrial & Engineering Chemistry Research* **2006,** *45* (19), 6477-6482.
6. Chen, Z.; Sun, Y., N-Halamine-Based Antimicrobial Additives for Polymers: Preparation, Characterization, and Antimicrobial Activity. *Industrial & Engineering Chemistry Research* **2006,** *45* (8), 2634-2640.
7. Akdag, A.; Worley, S. D.; Acevedo, O.; McKee, M. L., Mechanism of 5,5-Dimethylhydantoin Chlorination: Monochlorination through a Dichloro Intermediate. *Journal of Chemical Theory and Computation* **2007,** *3* (6), 2282-2289.
8. Chen, Y.; Worley, S. D.; Kim, J.; Wei, C. I.; Chen, T.-Y.; Santiago, J. I.; Williams, J. F.; Sun, G., Biocidal Poly(styrenehydantoin) Beads for Disinfection of Water. *Industrial & Engineering Chemistry Research* **2002,** *42* (2), 280-284.
9. Kocer, H. B.; Akdag, A.; Ren, X.; Broughton, R. M.; Worley, S. D.; Huang, T. S., Effect of Alkyl Derivatization on Several Properties of N-Halamine Antimicrobial Siloxane Coatings. *Industrial & Engineering Chemistry Research* **2008,** *47* (20), 7558-7563.
10. McCann, B. W.; Song, H.; Kocer, H. B.; Cerkez, I.; Acevedo, O.; Worley, S. D., Inter- and Intramolecular Mechanisms for Chlorine Rearrangements in Trimethyl-Substituted N-Chlorohydantoins. *The Journal of Physical Chemistry A* **2012,** *116* (26), 7245-7252.
11. Geerlings, P.; De Proft, F.; Langenaeker, W., Conceptual Density Functional Theory. *Chemical Reviews* **2003,** *103* (5), 1793-1874.